



Cite this: *RSC Adv.*, 2022, **12**, 31068

## Nanotechnology strategies for hepatocellular carcinoma diagnosis and treatment

WeiLu Jia, YingHui Han, XinYu Mao, WenJing Xu, a and YeWei Zhang\*

Hepatocellular carcinoma (HCC) is a common malignancy threatening human health, and existing diagnostic and therapeutic techniques are facing great challenges. In the last decade or so, nanotechnology has been developed and improved for tumor diagnosis and treatment. For example, nano-intravenous injections have been approved for malignant perivascular epithelioid cell tumors. This article provides a comprehensive review of the applications of nanotechnology in HCC in recent years: (I) in radiological imaging, magnetic resonance imaging (MRI), fluorescence imaging (FMI) and multimodality imaging. (II) For diagnostic applications in HCC serum markers. (III) As embolic agents in transarterial chemoembolization (TACE) or directly as therapeutic drugs. (IV) For application in photothermal therapy and photodynamic therapy. (V) As carriers of chemotherapeutic drugs, targeted drugs, and natural plant drugs. (VI) For application in gene and immunotherapy. Compared with the traditional methods for diagnosis and treatment of HCC, nanoparticles have high sensitivity, reduce drug toxicity and have a long duration of action, and can also be combined with photothermal and photodynamic multimodal combination therapy. These summaries provide insights for the further development of nanotechnology applications in HCC.

Received 16th August 2022

Accepted 20th October 2022

DOI: 10.1039/d2ra05127c

[rsc.li/rsc-advances](http://rsc.li/rsc-advances)

### 1 Introduction

Among cancers worldwide, liver cancer ranks seventh in incidence and second in mortality. The incidence rate is increasing

year by year.<sup>1</sup> Hepatocellular carcinoma (HCC) is the predominant form of liver cancer, accounting for about 90% of cases.<sup>2,3</sup> Some projections indicate that by 2025 there will be one million liver cancer patients per year worldwide.<sup>4</sup> Prevalence is generally higher in men than in women, and the risk is significantly increased in middle-aged and older (>40) people.<sup>5</sup> The most significant risk factor for the development of HCC is cirrhosis, of which hepatitis viruses (including hepatitis B and C) cause about 50% or more. Although, with the emphasis on antiviral therapy, the risk of infection has been reduced compared to before, patients with cirrhosis after viral clearance are still a high-risk group.<sup>6-8</sup> In addition, HCC due to alcoholic and non-

<sup>a</sup>Medical School, Southeast University, Nanjing 210009, China. E-mail: 230218500@seu.edu.cn

<sup>b</sup>Outpatient Department, The Second Affiliated Hospital of Nanjing Medical University, Nanjing 210009, China. E-mail: 406530357@qq.com

<sup>c</sup>Hepatopancreatobiliary Center, The Second Affiliated Hospital of Nanjing Medical University, Nanjing 210009, China. E-mail: symaoxinyu@163.com; zhangyewei@njmu.edu.cn

† These authors contributed equally to this work.



WeiLu Jia received his master's degree from GuiZhou medical University of China in 2020. Now he is a MD candidate at Southeast University, supervised by Prof. Yewei Zhang. Currently, his work focuses on drug delivery and Multimodal therapy for tumors.



Yewei Zhang earned his PhD degree from Suzhou University of China in 2005. In 2017, he joined the Southeast University. Then he joined The Second Affiliated Hospital of Nanjing Medical University, as a full professor. His current work focused on nanomedicine treatment for liver cancer.



alcoholic chronic liver disease (e.g. fatty liver, steatohepatitis) is increasing.<sup>9–11</sup> The early stage of limited HCC lacks obvious symptoms, while the clinical manifestations of advanced HCC include medium-sized liver and spleen, ascites, jaundice, anorexia, accompanied by weight loss, and upper abdominal discomfort and pain. HCC is highly aggressive and often metastasizes in distant organs such as lung and stomach.<sup>12–14</sup> Most cases are found to be advanced, and the prognosis and survival rate are extremely poor.<sup>15</sup> Despite our improved understanding of the pathogenesis and molecular level of HCC, the differences in its etiology and genetic mutations have led to poorer treatment outcomes.<sup>16–18</sup> Nowadays, the rise of nanotechnology can provide new ideas and methods for the early diagnosis and treatment of HCC.

Nanotechnology, mainly the modification of different nanoparticles (NPs), has been widely used in biomedical research, especially in oncology diagnostics.<sup>19</sup> NPs have many irreplaceable advantages; its small diameter makes it easy for the human body to metabolize; its large surface area allows it to load therapeutic drugs, increase the duration of drug action, improve the effect while reducing drug concentration and mitigate drug side effects.<sup>20–22</sup> Specific enrichment of NPs in tumor tissues is a prerequisite for nondestructive *in vivo* tumor diagnosis and targeted therapy. This is achieved by two main mechanisms, passive targeting, which exploits the enhanced penetration and retention (EPR) effect, and active targeting, which involves loading nanomaterials with recognition ligands for tumor marker molecules.<sup>23–25</sup> Low toxicity and biocompatible nanocarriers have also been the focus of research. For example, a biodegradable copolymer poly(lactic acid-ethanolic acid) (PLGA), has been approved by FDA (Food and Drug Administration, USA)/EMA (European Medicines Agency).<sup>26</sup> It produces the same byproducts (H<sub>2</sub>O and CO<sub>2</sub>) as normal human metabolism through ester bond hydrolysis of lactic and glycolic acids.<sup>27</sup> In addition, there are ultra-small size NPs with nanoenzyme functions that have anti-inflammatory, antioxidant and anti-tumor effects.<sup>28–31</sup>

Although NPs-loaded drug therapy can increase its efficacy, the effect of single treatment remains mediocre. Multimodal diagnostics (using light, sound, heat, *etc.*) greatly improves the diagnosis rate and treatment of tumors.<sup>32–35</sup> Herein, this paper reviews the progress of nanotechnology application for HCC in recent years, which opens up new areas for early diagnosis, improved efficacy and prolonged survival of HCC (Fig. 1).

## 2 Diagnosis

### 2.1 Imaging

**2.1.1 Computed tomography (CT) and positron emission tomography (PET).** CT is a common imaging test for hepatocellular carcinoma.<sup>36,37</sup> Since the main source of blood supply for hepatocellular carcinoma differs from that of normal liver tissue, with the former being the hepatic artery and the latter being mainly the portal vein, enhancement of the arterial phase and fading of the delayed phase will occur in contrast imaging. It has a sensitivity of about 80% and a specificity of over 90% for the diagnosis of HCC.<sup>38,39</sup> Iodine compounds have a high X-ray

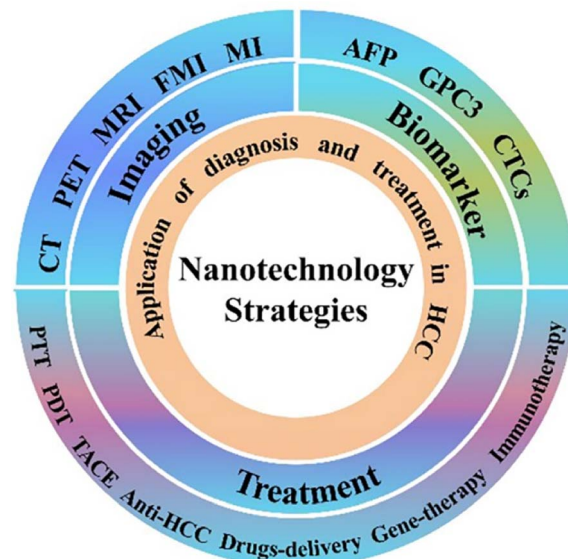


Fig. 1 Nanotechnology strategies for hepatocellular carcinoma.

absorption coefficient and are currently commonly used contrast agents for CT. However, hypertonic iodine contrast agents increase the burden on the kidneys when metabolized, and a small number of patients are allergic to iodine contrast agents.<sup>40</sup> It has been shown that the sensitivity and resolving power of CT for HCC are related to the contrast concentration.<sup>41</sup>

In recent years, the advent of nano-CT contrast agent overcomes the shortcomings of conventional contrast agents. Nano-contrast agents are modified to make them persistent and specific in imaging HCC. Kim *et al.* reported a polyethylene glycol (PEG)-coated gold-based NPs (GNPs) with a diameter of approximately 30 nm that had a long retention time in the blood compared to iodine contrast agents. Moreover, because gold has a higher absorption coefficient than iodine, the CT contrast between normal liver tissue and tumor was improved 2-fold after injection of GNPs in the tail vein of tumor-bearing

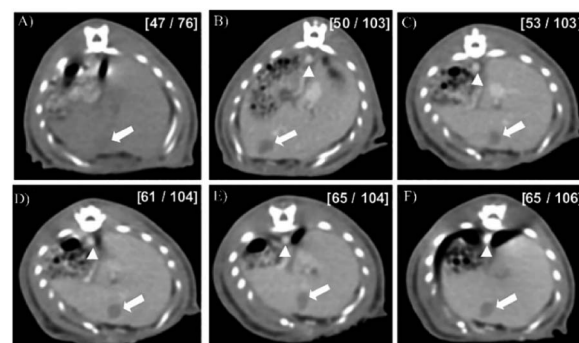


Fig. 2 CT images of rat HCC model after injection of GNPs. Images were obtained at (A) 0 h (before injection) and (B) 5 min, (C) 1 h, (D) 2 h, (E) 4 h, and (F) 12 h after injection. Numbers in brackets are the HU values of the hepatoma regions (left) and the surrounding normal liver parenchyma (right). Reproduced with permission from ref. 38. Copyright American Chemical Society, 2007.



rats<sup>42</sup> (Fig. 2). Based on the above study, Rand *et al.* used a layer-by-layer coating method of polyelectrolytes to coat anionic polyacrylic acid and cationic polypropylene amine hydrochloride on GNPs layer by layer to increase the affinity of GNPs with cells and reduce their concentration at the time of use.<sup>43</sup> Meanwhile, the application of spatial harmonic imaging (SHI) to the images formed by X-ray scattering improved the accuracy of detecting HCC cells down to several millimeters in diameter.<sup>43</sup> For now, the cost of gold-based nanoparticles may be higher than that of iodine-based contrast media, especially in developing countries, which is difficult to apply. It is believed that a balance between efficacy and price will be found in the near future.

Micro-CT is a non-invasive imaging tool commonly used in rodents. It helps us to perform preclinical experiments on animal models.<sup>44</sup> A team of researchers used micro-CT on liver cancer model mice to compare the effects of two alkaline earth metal nanocontrast agents, Exitron nano 6000/12 000. These two contrast agents target hepatic Kupffer cells and have the advantage of high contrast and long duration (>4 h). In particular, the extended contrast of Exitron nano 12000 on the hepatic vascular system enables semi-automatic segmentation of the liver and tumor, providing a dynamic monitoring method for quantitative estimation of HCC load.<sup>45</sup> Encouragingly, Anton *et al.* developed a completely non-toxic 2-3-5-triiodo- $\alpha$ -tocopherol ( $\alpha$ -tocopherol is vitamin E) contrast emulsion to achieve

quantification of micro HCC detection and volume and to stay in the liver for 3 months.<sup>46</sup> (Fig. 3) In addition, a labeled human serum albumin microspheres (HSAM) was used for imaging and became effective after 2 h and remained stable in the liver after 72 h.<sup>47</sup>

PET uses positron nuclide labeling of body metabolites such as glucose as the imaging agent and reflects metabolic changes through the uptake of the imaging agent by the lesion, thereby detecting microscopic tumors and invasive metastases of tumors and providing a high spatial resolution.<sup>48</sup> PET is a second-line option for HCC diagnosis.<sup>49,50</sup> Some research teams have modified liposomes (LPs) and radionuclides at the nanoscale to target imaging ligands to diseased tissues or organs using their specific targeting effects, thereby increasing the image signal/contrast of the target tissue at lower concentrations.<sup>51</sup> Unfortunately, there are few reports on the direct application of these nanoscale modifications in the diagnosis of HCC. The possible reason is that PET can play a greater advantage in the diagnosis of distant metastasis of tumor. Usually, it is difficult to recommend animal models of tumor metastasis, which may be a direction for future research and development.

**2.1.2 Magnetic resonance imaging (MRI).** MRI is not only non-radioactive, but also more specific than CT in the diagnosis of HCC.<sup>1,52</sup> However, the sensitivity and specificity of conventional MRI diagnosis are still unsatisfactory. Gadolinium diethylenetriamine pentaacetic acid (Gd-DTPA) is a commonly used contrast agent in clinical practice, but it has a short half-life in the blood and lacks specificity for the target tissue. In

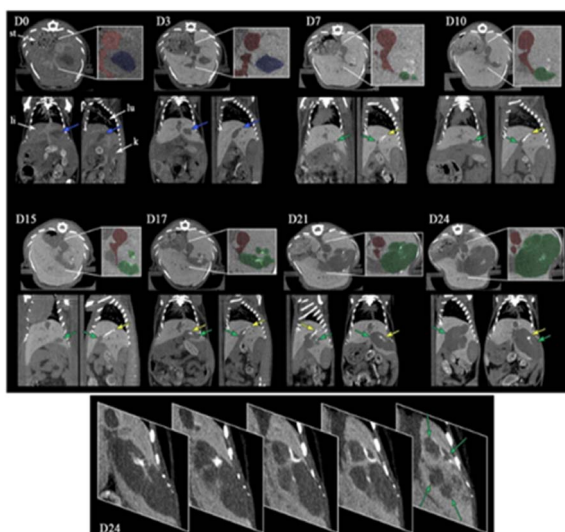


**Fig. 3** Micro-CT imaging of tumor-bearing mice after intrahepatic injection of  $\alpha$ -tocopherol nanoemulsion and the pictures report maximum intensity projection of transverse section, sagittal and coronal section of the liver, for 0, 3, 7, 10, 15, 17, 21 and 24 days after injection of the cells and iodinated nano-emulsions as contrast agent. At D0, are indicated in the figure the localizations of the stomach (st), liver (li), lung (lu) and kidney (k). Insets show details with colored filters that guide the eye to differentiate the vascularization (in red), cell injection cavity (in blue), and tumor (in green), completed by arrows in the other views. Yellow arrows point out the hyper-contrast zones that appear during the tumor growth. The bottom part, at D24, shows transverse sections of tumor for different depths, emphasizing the different tumor nodules with green arrows.

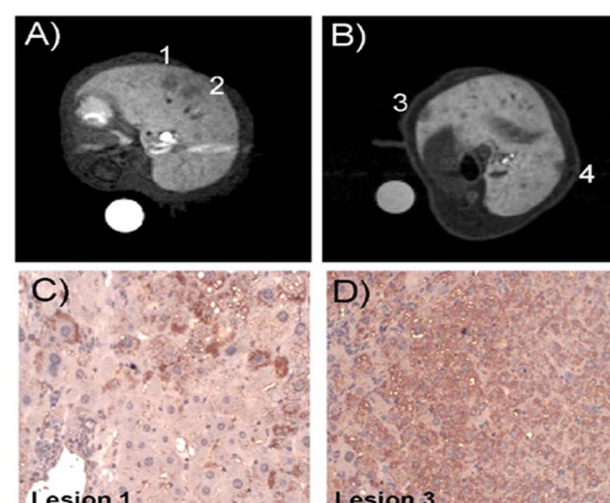


**Fig. 4** Histological validation of MRI lesion detection. T1-weighted MR images (liver region), of HBV-Tg transgenic mice 20 min after the injection of Mn-Apo (A) and Gd-BOPTA (B), respectively. Lesions 1 and 2 were easily detectable only after Mn-Apo administration. However, lesions 3 and 4 were detectable only after Gd-BOPTA injection. (C and D) Expression pattern of SCARA5 in HBV-Tg. (C) Immunohistochemical staining of lesion 1 showing low Mn-Apo uptake. SCARA5 was observed only in some HCC cells. (D) Immunohistochemical staining of lesion 3 showing higher Mn-Apo uptake. SCARA5 was present in almost all cancer cells. Reproduced with permission from ref. 50. Copyright John Wiley & Sons, Ltd, 2012.



this regard, Chen *et al.* achieved longer retention and better results in HCC imaging by assembling the contrast agent with polylactic acid (PLA)-PEG in a nanocomplex.<sup>53</sup>

In addition to Gd-based contrast agents, Manganese may be a potential metal to replace Gd. Researchers have developed an Mn-based contrast agent encapsulated in apoferritin (Mn-Apo), which exhibits different high and low T1 weighting signal intensities due to its different proportions in hepatocytes and HCC cells. In addition, further studies have shown that Mn-Apo cellular uptake correlates with SCARA5 (an oncogenic molecule) receptor expression, and using SCARA5 as a molecular marker for HCC, other invisible lesions can be detected by Mn-Apo<sup>54</sup> (Fig. 4).

Moreover, manganese conjugated nanodiamond complexes improve the interaction between paramagnetic ions and water molecules, thus improving MRI vertical (T1) and horizontal relaxation (T2).<sup>55</sup> 3,4-Dihydroxycinnamic acid-functionalized superparamagnetic iron oxide nanoparticles (IONPs) are biocompatible and can produce significant contrast enhancement in T2 weighting.<sup>56</sup> Nano bullets (Mn-DTPA-F-MSNs) coupled with mesoporous silica nanoparticle (MSN) were able to detect glutathione (GSH) along with the enhancement of MRI.<sup>57</sup>

**2.1.3 Fluorescence molecular imaging (FMI).** More than two-thirds of patients who have undergone hepatectomy for HCC develop tumor recurrence after 5 years, and the possible cause is often explained by complete resection of the tumor

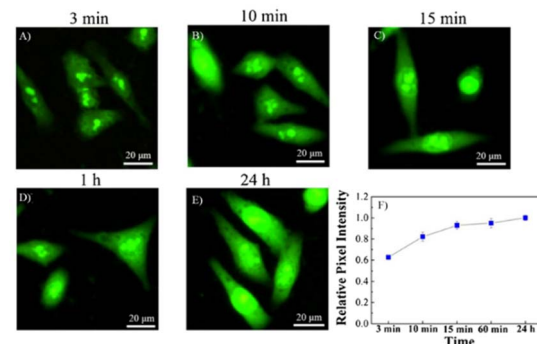


Fig. 6 Fluorescence images of HepG2 cells after incubating with appropriate medium containing Cdots for different time ((A) 3 min, (B) 10 min, (C) 15 min, (D) 1 h, (E) 24 h). (F) Relative pixel intensity of the corresponding fluorescence images (the pixel intensity from HepG2 cells incubated with Cdots for 24 h was defined as 1.0).

lesion.<sup>58</sup> The FMI-guided surgery helped the surgeon preserve a greater degree of normal liver tissue and remove the tumor lesion intact.<sup>59,60</sup> A commonly used fluorescent probe in clinical practice is indocyanine green (ICG), which aggregates in HCC tissue and emits near-infrared light upon activation.<sup>61</sup> Currently, the two main limitations of ICG fluorescence imaging in HCC surgery are the limited depth of tissue penetration (<10 mm) and the false positive rate (45%).<sup>62,63</sup> To overcome these shortcomings, the nano-flower particles formed by the combination of SiO<sub>2</sub> coated Au and antibody have stronger tissue penetration and luminescence properties.<sup>64</sup> A novel europium oxide nanoparticle mediate fluorescent images from emissive drugs and detect even ultra-small tumors below 1 mm.<sup>65</sup> (Fig. 5) Cdots developer rapidly penetrate the membrane of HCC cells and maintain its position for 24 h, emitting a bright green fluorescence different from that of normal hepatocytes<sup>66</sup> (Fig. 6).

Recent studies have found that viscosity maintains one of the parameters of microenvironmental homeostasis in organisms, and its abnormal changes can lead to the development of many diseases, such as tumors and diabetes.<sup>67</sup> In response to the significantly higher viscosity in hepatocellular carcinoma cells, Li *et al.* developed a fluorescent probe specific for hepatocytes (HT-V) that not only allows bioimaging but also sensitively detects differences in viscosity for *in vivo* diagnosis of HCC.<sup>68</sup>

Furthermore, Surface-Enhanced Raman scattering (SERS) has been reported to be more sensitive and photostable than fluorescence imaging. The ability of Raman imaging of SERS NPs to detect HCC is more accurate and stable than that of ICG.<sup>69</sup>

**2.1.4 Multimodal imaging.** Both CT and MRI have limitations in diagnosing swelling, such as penetration depth and specificity.<sup>70</sup> Nanotechnology-based multimodal imaging combines the advantages of two or more imaging modalities to compensate for the shortcomings of a single imaging modality, providing a more accurate method for the diagnosis of HCC.<sup>71,72</sup> Folic acid (FA) combined with Gd functionalization to form nanodroplets (Gd-NDs-FA) accumulate within the tumor area

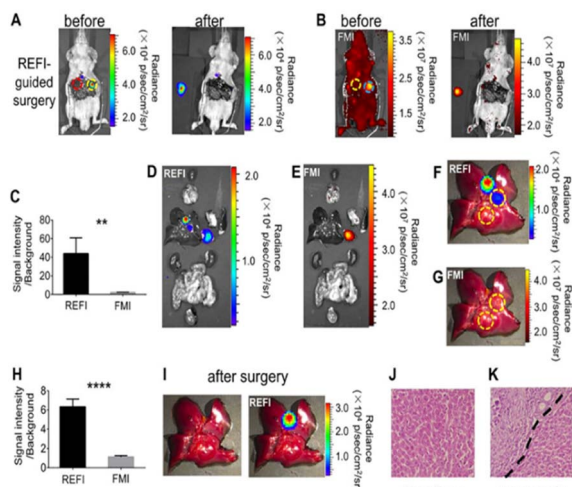


Fig. 5 REF image-guided cancer surgery of the orthotopic HCC tumor-bearing mice. (A) Representative REF of the mouse after the laparotomy (left). After the REF image-guided cancer surgery, the mouse and the resected tumor were also imaged for REF (right). (B) Representative fluorescent images of the mouse before and after the tumor resection. (C) Comparison of SNR of REF and FMI. (D) and (E) REF and FMI of all the organs and the orthotopic HCC. (F) and (G) Representative REF and FM image of the mouse liver, respectively. (H) Comparison of quantification of SNR of REF and FMI of the mouse liver. (I) Photograph and REF image of the mouse liver after the tumor second resection, respectively. (J) and (K) H&E of the orthotopic HCC and surgical margin, respectively. Reproduced with permission from ref. 61. Copyright Elsevier Inc, 2017.



and exhibit intense ultrasound (US) and MRI signal enhancement.<sup>73</sup> A novel nanoprobe formed by HCC-targeting peptide, NIR dye and Gd chelation with enhanced fluorescence and MRI dual-mode imaging for intraoperative detection of lesions smaller than 1 mm.<sup>74</sup> Similarly, a rare-earth-doped NPs (dREs@Lips) has the same function.<sup>75</sup> Cationic straight-chain starch (CA) and superparamagnetic iron oxide (SPIO) NPs modified to form nanospheres and loaded with small interfering RNA (siRNA) exhibited both good fluorescence and magnetic resonance imaging properties as well as inhibition of HCC growth.<sup>76</sup> In addition, a multifunctional PEG-Ta<sub>2</sub>O<sub>5</sub>@CuS nanoprobe was designed to enhance gemstone spectral computer tomography (GSCT) and photoacoustic (PA) imaging while allowing ablation of HCC.<sup>77</sup>

Ultrasonography is a routine tool for HCC screening, and unfortunately, the use of NPs in HCC ultrasonography has not been reported compared to other imaging examinations.

## 2.2 Serum biomarkers

**2.2.1 Alpha-fetoprotein (AFP).** AFP is one of the most commonly used markers for the diagnosis of HCC. Although some studies have shown that less than 20% of HCC patients have an AFP level of 400 ng mL<sup>-1</sup>, the combination of AFP testing and imaging greatly improves the accuracy of diagnosis.<sup>78</sup> In addition, AFP testing can help in managing the treatment process and predict the prognosis of patients with HCC.<sup>79,80</sup> Traditional methods (e.g. enzyme-linked immunosorbent assay, ELISA) for the detection of AFP have disadvantages

such as low sensitivity, complex and time-consuming operation, and expensive equipment and consumables.<sup>81,82</sup>

Over the past decade, a number of low cost, efficient and rapid AFP assays based on nano-strategies have been developed.<sup>83-85</sup> They usually use electrochemiluminescence (ECL) and electrochemiluminescence immunoassays for the detection and quantification of markers.<sup>86,87</sup> Metal nanoparticles, especially gold-based nanoparticles, are usually hybridized with other nanomaterials to make biosensors for detecting AFP. NPs assembled in nano-hydroxyapatite prepared piezoelectric immunosensor for highly sensitive detection by immunoreactivity.<sup>88</sup> The combination of Fe<sub>3</sub>O<sub>4</sub>-Au and CdS-Au NPs into a sandwich core ECL immunosensor has the advantages of magnetic separation and the stability and biocompatibility of Au, with a detection range of 0.0005 ~ 5.0 ng mL<sup>-1</sup>.<sup>89</sup> Organic NPs, such as carbon nanotubes, quantum dots, and graphene, have applications in this area as well.<sup>83,90</sup> Similarly, other non-metallic nanoparticles (e.g. silica NPs) are also widely used in the fabrication of biosensors.<sup>85</sup> Herein, we have selected some representative NPs to summarize (Table 1).

**2.2.2 Glycican-3 (GPC3).** GPC3 is a polysaccharide molecule that is highly expressed in HCC.<sup>109</sup> It can be released into the serum and is an emerging serum marker for HCC diagnosis.<sup>110,111</sup> To improve its accuracy, the researchers developed nano-luciferase with dual functionality to detect trace amounts of GPC3 in serum.<sup>112</sup> In addition, attaching specific peptides to gold nanoparticles can be used as a probe to detect GPC3 specificity.<sup>113</sup>

Table 1 Different NPs in detecting AFP<sup>a</sup>

Category	Types of nanoprobe	Detection method	Ref.
Metal-based	Ru-silica@Au	CV and ECL	91
	Ferrocenemonocarboxylic-HRP@Pt	Multiple amplification immunoassay	92
	Fe <sub>3</sub> O <sub>4</sub> -Au/Ab1/AFP/Ab2/CdS-Au	ECL	89
	Au Pt NPs\HRPNPs\NiHCF NPs	ECL	84
	GNMA	LSPR/iImmunoassay	93
	Pd/APTES-M-CeO <sub>2</sub> -GS	ECL	94
	Multi-HAT-AuNP-Ab2	ELISA	95
	Met-Au NCs	ECL	96
	GNTC	LSPR/enzymatic precipitation	97
	GNA	LSPR/enzymatic precipitation	98
	MIL-101(Cr) & CdSe QDs	PEC	99
	MoS <sub>2</sub> /Au NPs	Love-mode SAW	100
	GCE/3D-Cu-Flo. @AuNPs-Cys	3D-ECL	101
	SnO <sub>2</sub> Nanotubes	PEC	102
Organic	GO-HRP	Immunoassay	90
	MWCNT	Colorimetric and chemiluminescent assays	103
	Multicolor QDs	Immunoassay	104
	Si NPs/SiC@Ag	SERS	105
Nanocomplexes	g-C <sub>3</sub> N <sub>4</sub> @TiO <sub>2</sub> NTs	PEC	106
	GCE/CNTs-gC <sub>3</sub> N <sub>4</sub> (Cu)	ECL	107
	ZIS	3D-AIO/PEC	108

<sup>a</sup> CV: cyclic voltammetry; HRP: horseradish peroxidase; NiHCF: nickel hexacyanoferrate; LSPR: localized surface plasmon resonance; GNMA: gold nano-m arrays; Pd/APTES-M-CeO<sub>2</sub>-GS: 3-aminopropyltriethoxysilane supported Pd octahedral nanoparticles; HAT: human alpha-thrombin; Met-Au NCs: methionine-stabilized Au nanoclusters; GNTC: gold nano-truncated cone; GNA: gold nanodot array; PEC: photoelectrochemical; CNT: carbon nanotube SAW: surface acoustic wave; Cu-Flo. NMs: copper-based nanosheet micromaterial; Cys: cysteine; GCE: glassy carbon electrode; ZIS: ZnIn<sub>2</sub>S<sub>4</sub>; 3D-AIO: 3D printing all-in-one dual-modal immunoassay.



**2.2.3 Circulating tumor cells (CTCs).** Metastatic spread of tumors is usually reported from CTCs, which are shed from the primary tumor through the hematologic route and colonize distant tissues.<sup>114</sup> A large amount of predictive, disease progression information for HCC can be obtained by detecting CTCs in peripheral blood, providing reliable evidence for clinical diagnosis and individualized treatment evaluation.<sup>115</sup> Because CTCs are extremely rare in blood, the specificity and accuracy of epithelial cell adhesion (EpCAM)-coated magnetic bead isolation assays are often inadequate for clinical applications.<sup>116</sup> Xia *et al.* modified  $\text{Fe}_3\text{O}_4$  nanobeads with small molecule NIR fluorophore MLP and EpCAM antibody with dual-mode selection and separation, which greatly improved the capture efficiency and detection purity of CTCs<sup>117</sup> (Fig. 7). Similarly, a composite nanoparticle with  $\text{Fe}_3\text{O}_4$  magnetic cores encapsulated in an anti-EpCAM-modified MIL-100 shell layer can be automatically degraded by MIL in an acidic environment, resulting in high activity of the captured CTCs.<sup>118</sup> Reassuringly, a dual-targeted functionalized reduced graphene oxide membrane (DTFGF) detects as low as 5 HCC-CTCs in 1 mL of blood sample.<sup>119</sup> It is foreseen that the application of nanotechnology in HCC-CTCs has this great potential.

### 3 Treatment

In patients with HCC, different tumor stages and patients' own nutritional status require individualized treatment plans. Clinically, the most commonly used staging system is the

Barcelona Clinic Liver Cancer (BCLC) staging system, which guides the selection of different treatment options based not only on tumor growth and invasion, but also on liver function and overall physiological status.<sup>120,121</sup> In the early stages of HCC, surgical resection, liver transplantation and ablation can be used. In the intermediate stage, local treatments, such as transarterial chemoembolization (TACE), are mainly used. In the late stage, systemic systemic therapy such as targeted therapy and immunotherapy are used. These treatments improved the course of each stage of the disease and increased the 5 year survival rate.<sup>122,123</sup> Unfortunately, HCC is usually diagnosed at an advanced stage and treatment outcomes remain unsatisfactory. The treatment modalities and new drugs are constantly being explored and improved, and the application of nanotechnology has opened up a promising solution in which nanoparticles are designed into targeted, highly efficient regimens that provide personalized, precise treatment modalities.

#### 3.1 Thermal ablation and photothermal therapy (PTT)

Ablation technique is the preferred method to treat early stage small HCC (especially  $<2$  cm, single tumor), which is tumor necrosis by thermal and chemical methods.<sup>124</sup> At present, two thermal ablation techniques, radiofrequency ablation (RFA) and microwave ablation (MWA), are more commonly used in clinical practice.<sup>125</sup> The researchers focused on the improvement of the thermal ablation probe to achieve better treatment results. Shao *et al.* compared three nanoparticles CNT, Au and

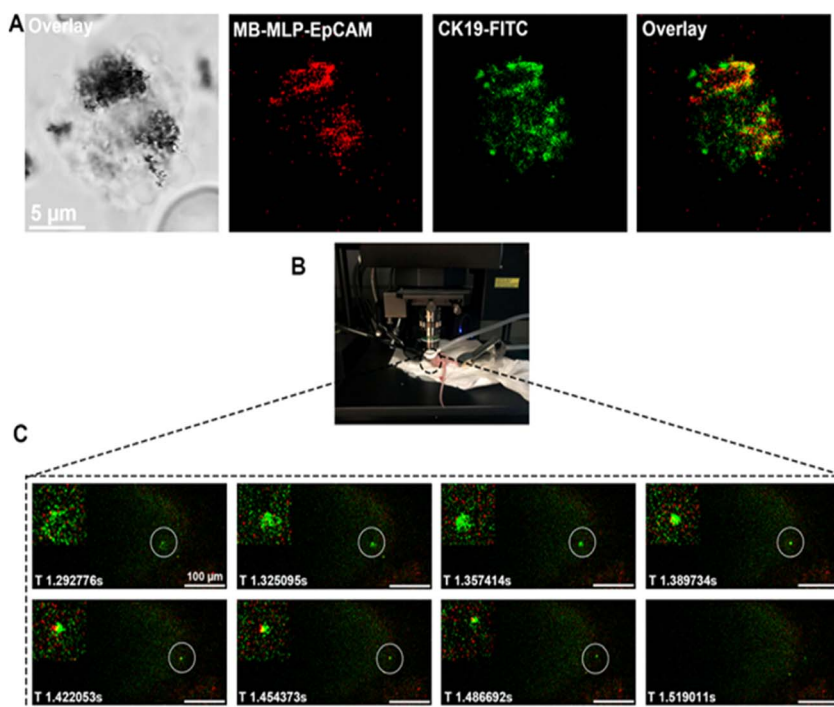


Fig. 7 (A) Fluorescent images of the CTC captured by MB-MLP-EpCAM from clinical blood samples of HCC patients. The red fluorescence represents MB-MLP-EpCAM, and the green fluorescence represents CTC (CK19+). (B) the mouse fixation and imaging diagram. (C) Recognition of MB-MLP-EpCAM for GFP transfected HepG2 cells *in vivo* at different time points. Reproduced with permission from ref. <sup>113</sup>. Copyright American Chemical Society, 2020.



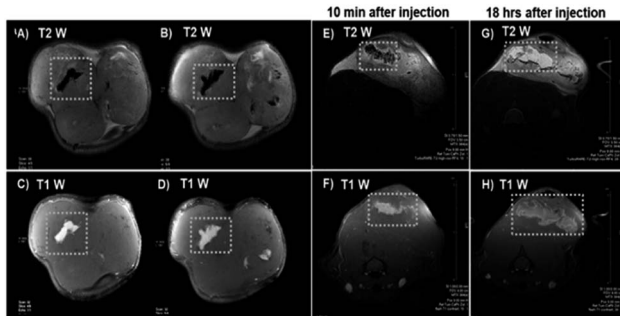


Fig. 8 Dual T1–T2 contrast variation after intra-tumoral injection. (A and B) T2 weighted and (C and D) T1 weighted MR image (coronal section) of subcutaneous tumor after intratumoral nCP: Fe injection. (E) T2 weighted and (F) T1 weighted MRI of subcutaneous tumor (axial sections) 10 min after intratumoral injection of nCP: Fe. (G) T2 weighted and (H) T1 weighted MRI of subcutaneous tumor (axial sections) 18 hours after intratumoral injection of nCP: Fe. Sample injected regions are shown in white dotted boxes.

$\text{Fe}_3\text{O}_4$  as therapeutic probes for RFA. These probes have higher heat transfer efficiency and lower maximum temperatures, with a more uniform temperature distribution in the CNT.<sup>126</sup> A single-phase calcium phosphate biomimetic NPs for contrast imaging under MRI to guide RFA.<sup>127</sup> (Fig. 8) In addition, *in vivo* excitation of nano-hydroxyapatite solutions with high-intensity ultrasound enhances thermal ablation and has a higher biosafety profile.<sup>128</sup> Recurrence after ablation therapy is also a rather difficult problem.<sup>129</sup> Mannose-derived carbon dots (Man-CDs) can effectively capture tumor-associated antigens and other risk factors after MWA treatment, induce body-specific immune responses, and maintain long-term immune effects to inhibit HCC recurrence.<sup>130</sup>

PTT is a recent technique to thermally ablate local tumors by converting light energy into heat through photothermal converters.<sup>131</sup> For PTT treatment of HCC, selective uptake of photothermal agents in liver tumor cells, photothermal conversion efficiency and biosafety have been hot topics of research. Metals and metal sulfides NPs are highly efficient photothermal agents. Their biotoxicity is reduced by their

encapsulation or modification. Graphene oxide (MGO) has become a hot research topic due to its low biotoxicity, large specific surface area and efficient photothermal conversion efficiency. For example, encapsulation of gold nanorods (AuNRs) inside graphene oxide NPs (NGO) or mesoporous silica shells to form nanocapsules for improved safety and photothermal conversion efficiency.<sup>132–134</sup> Similarly, Wen *et al.* successfully constructed an organic-inorganic hybrid nanomaterial (MGO@CD-CA-HA) by encapsulating  $\beta$ -cyclodextrin-cholic acid-hyaluronic acid polymer (CD-CA-HA) on FeO-MGO. It has high efficiency in photothermal conversion efficiency along with multi-targeting for HCC.<sup>135</sup> Copper sulfide wraps hollow spheres with membrane proteins from tumors and macrophages, which can also be loaded with therapeutic agents inside, creating a multimodal treatment for HCC.<sup>136</sup> There are also some metal oxides, *etc.* that have been processed by bionic means and have shown the powerful therapeutic potential of PTT. We have summarized the commonly used photothermal agents and modifications.

### 3.2 Photodynamic therapy (PDT)

PDT is also a form of ablative treatment for HCC, which has the advantages of less trauma, shorter treatment time, lower side effects and higher repeatability.<sup>137</sup> PDT kills tumor cells, destroys tumor blood vessels and stimulates activation of the immune system through reactive oxygen species (ROS), including superoxide anions and free radicals, produced by light-activated photosensitizers (PSs).<sup>138,139</sup> Some conventional PSs have many problems such as low ROS generation efficiency and lack of targeting.<sup>140</sup> The class of PSs includes organic PSs (*e.g.* porphyrins), natural products, metal complexes, metal-organic backbones (MOFs), and metal-based nanostructures.<sup>141</sup> In addition, some researchers have modified PSs by FA or HA to make tumor-targeting probes, thus further improving their tumor specificity and water solubility.<sup>142</sup> The nano-strategy overcome the above disadvantages, and NPs target PSs delivery to HCC cells through EPR effect, which also enhance the effect of PDT.<sup>143</sup> Photo-sensitive sulfated zinc phthalocyanine loaded on nanoliposomes significantly enhances the

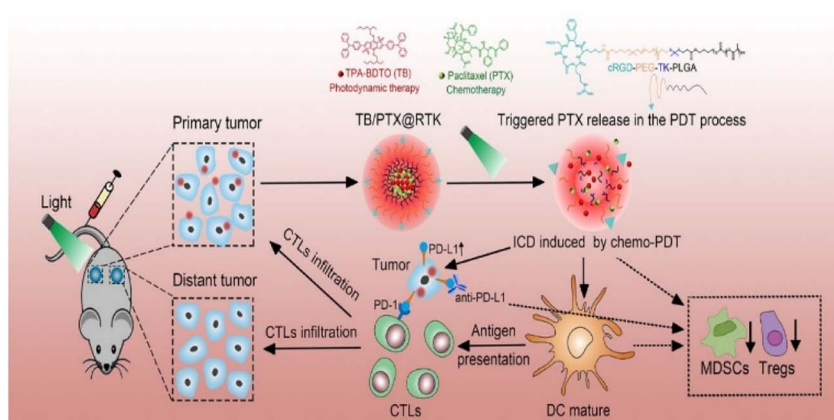


Fig. 9 All-in-one multimodal nanotherapy platform.



accumulation in HCC cells.<sup>144</sup> Similarly, Xu *et al.* developed a light-triggered nanomicellar beam delivery platform loaded with PSs and paclitaxel (PTX), which not only has the effect of PDT with chemotherapy, but also synergizes with anti-PD-L1 antibody for immunotherapy.<sup>145</sup> (Fig. 9) In addition, novel PSs (PS-GNPs) formed by the combination of Pu-18-N-butylimide-NMGA and chloroauric acid in a mouse model of hepatocellular carcinoma showed upregulation of ROS-associated apoptosis proteins and increased DNA fragmentation.<sup>146</sup> From polygalactose-co-cinnamaldehyde polyexcipients (PGCA) and the photosensitizer pheophorbide A self-assembled into PGCA@PA NPs, the uptake of NPs by tumor cells was facilitated by the expression of galactose receptors, while the combination of the two enhanced the PDT.<sup>147</sup>

### 3.3 TACE

TACE is a minimally invasive approach to treat unresectable HCC. Chemotherapeutic agents and embolic agents are injected into the hepatic artery to reduce the blood supply to HCC and induce necrosis. However, the efficacy of TACE is unsatisfactory, and although drug-eluting beads (DEBs) are used, there are still problems with its low response rate, as well as chemotherapeutic drug escape and tumor drug resistance.<sup>148-150</sup> In response, Kong and his colleagues used Arsenic trioxide

(ATO) encapsulated in biocompatible PLGA for TACE with strong tumor suppressive effects.<sup>151</sup> A novel binary progressive micro- and nanostructured embolic microspheres were developed for application in TACE, which have good swelling properties and both tumor embolization and inhibition of tumor angiogenesis.<sup>152</sup> MnO<sub>2</sub>/vitraphen (BPD) nanocomposites as embolic agents to promote tumor vascular endothelial cell apoptosis and predict treatment efficacy by showing tumor vascular density through multimodal imaging<sup>153</sup> (Fig. 10).

Furthermore, nanosized modifications of chemotherapeutic or targeted drugs are also used directly for TACE treatment. Nanosized PTX or sorafenib (SRF) not only improves the chemotherapeutic effect, but also increases the safety without introducing additional carriers.<sup>154,155</sup> Wang *et al.* developed magnetic liquid metal NPs (Fe@EGaIn) loaded with calcium alginate (CA) microspheres with CT/MR dual-mode imaging in addition to embolization and drug coating functions.<sup>156</sup> The flexibility and multiple functionalization of this microsphere provides a template for future development strategies.

### 3.4 Direct anti-HCC effect of NPs

From the current literature, some NPs act directly on tumor cells to induce apoptosis. For example, direct treatment of HCC with selenium NPs may act by regulating DNA methylation,

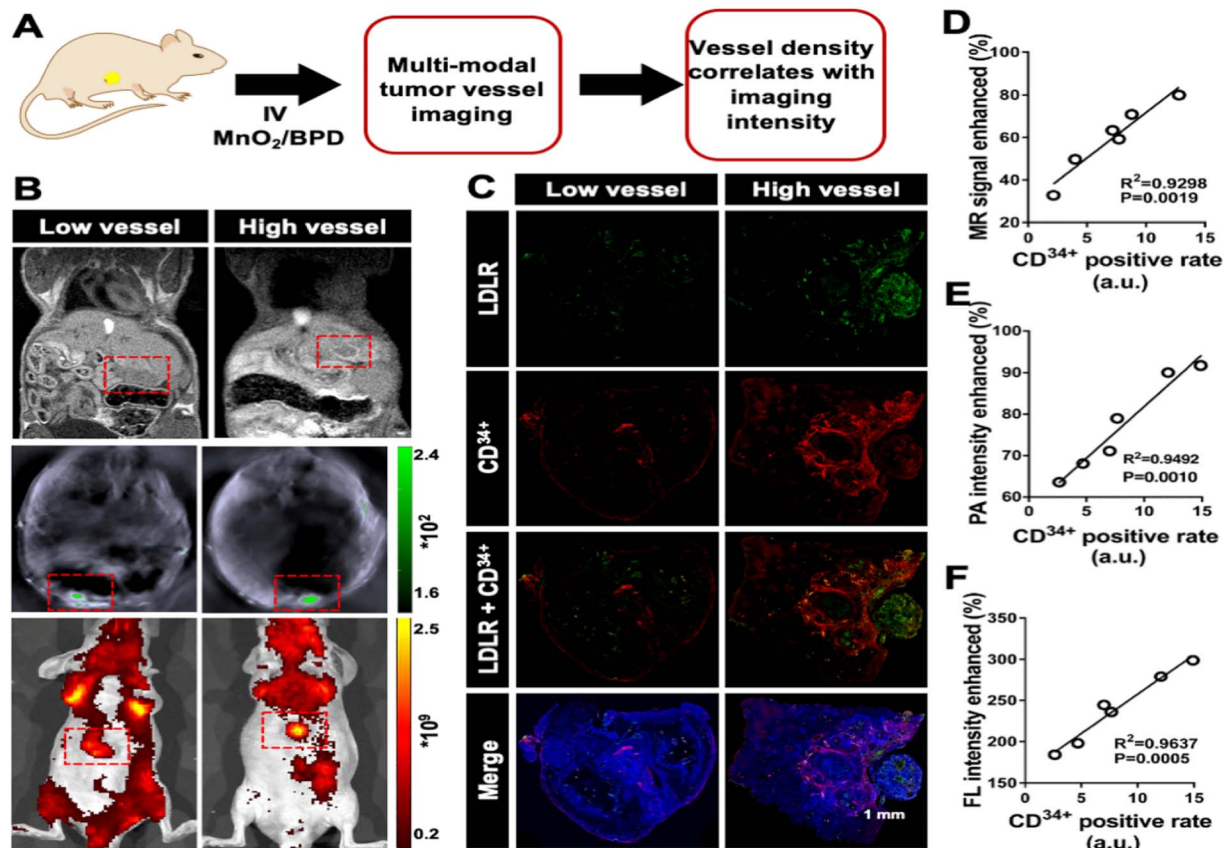


Fig. 10 Vessel density imaging predicts embolization effect. (A) Experimental design. (B) Example of MR, PA, and FL images of hep-G2 tumors presenting low and high vessel intensity. (C) Whole slice imaging of immunofluorescence. (D) Linear regression between vessel density and MR signal enhancement. (E) Linear regression between vessel density and PA intensity enhancement. (F) Linear regression between vessel density and FL intensity enhancement. Reproduced with permission from ref.<sup>146</sup>. Copyright American Chemical Society, 2020.



where the molecular mechanisms include: (a) reduced the ratio of 8-OHdG/2-dG production to avoid DNA damage caused by oxidative stress, (b) upregulated the expression of two onco-genes, *Akr1b10* and *ING3*, and (c) significantly reduced the expression of *Foxp1* gene.<sup>157</sup> AgNPs promotes caspase-3 (signaling pathway is p53, AKT and MAPKs) to participate in cell apoptosis through ROS generation.<sup>158</sup> Moreover, AgNPs also reduce the protective effect of liver related biochemical indexes, such as aspartate transaminase (AST) and gamma glutamyl-transpeptidase (GGT).<sup>159</sup> Nano  $\beta$ -TCP not only induced apoptosis through ROS, but also blocked the G0/G1 cell cycle of HCC cells and interfered with the expression of cyclin.<sup>160</sup> Niu *et al.*, through bioinformatics analysis, found that nano-sio<sub>2</sub> can up-regulate tumor cell-related death gene ZBP-1, which has a killing effect on HCC cells.<sup>161</sup> Other research teams have also found that NPs such as AgO<sub>2</sub>, CeO<sub>2</sub> and CuO<sub>2</sub> have HCC-killing effects, but their molecular mechanisms are not yet clear.<sup>162</sup>

### 3.5 NPs for delivery of drugs

**3.5.1 NPs for delivery of chemotherapeutic drugs.** Different chemotherapeutic drugs were modified with nanotechnology to form functionalized NPs with stronger targeting and efficacy. Doxorubicin (DOX) encapsulated in biological metal organic frameworks (MOFs) is biologically low in toxicity and can be precisely administered.<sup>163</sup> In addition, nigella sativa oil and DOX formed nanoemulsifiers with lower tumor-inhibiting concentrations, mitigating DOX toxicities and providing a reference for further oral administration.<sup>164</sup> A polymeric micelle capable of rapid mucus penetration and villi absorption

allows effective delivery of PTX into HCC by oral administration.<sup>165</sup> A novel sulfhydryl polymer-based nanocomposite loaded with 5-fluorouracil (5-FU) reduces serum levels of liver enzymes in addition to targeting of HCC.<sup>166</sup> Moreover, chemotherapeutic drugs such as cisplatin (CDDP) and ceramide have been nano-engineered.<sup>167</sup> Herein, our team summarize the commonly used chemotherapeutic drug nanoparticles in recent years (Table 2).

#### 3.5.2 NPs for delivery of molecularly targeted drugs.

Chemotherapeutic drugs are less effective and have more pronounced toxic side effects in HCC, especially in mid-to late-stage progressive HCC.<sup>178</sup> Molecularly targeted drug therapy, which is the first and second line of treatment, is commonly used in clinical practice today. First-line drugs such as sorafenib (SRF) and lenvatinib (LEN) are multiple receptor tyrosine kinase inhibitors (TKIs) that can improve overall survival.<sup>179</sup>

However, their effects are limited by their side effects and low bioavailability.<sup>180</sup> Peptide nanogels with stimulatory response were developed for LEN delivery with good tumor suppression effect and few side effects.<sup>181</sup> LPs carrying SRF and ganoderic acid are used as anti-HCC agents. They significantly inhibit tumor growth and inflammatory factors, as well as reduce liver enzyme levels.<sup>182</sup> Mn-doped silica NPs loaded with SRF double deplete intracellular glutathione (GSH) and thus disrupt redox homeostasis in HCC cells.<sup>183</sup> In addition, PEG galactose-coupled nanosolid lipid-loaded SRF has better pharmacokinetics and hepatic targeting.<sup>184</sup>

**3.5.3 NPs for delivery of natural plant medicine.** Natural plant drugs are used for anti-HCC treatment because of their low toxicity, but most of them have poor water solubility that limits their wide application.<sup>185</sup> Curcumin (CU) is an anti-inflammatory and anti-cancer natural polyphenolic plant component with enhanced solubility and anti-cancer effects, which was modified into nano vesicles by Abbas *et al.*<sup>186</sup> Similarly, CU mitochondrial delivery system based on polyamide dendrimer molecules increase mitochondrial ROS levels and induce apoptosis at lower doses.<sup>187</sup> GA LPs interfere with various signaling proteins involved in HCC pathogenesis, altering.

Table 2 Different NPs for delivery of chemotherapeutic drugs<sup>a</sup>

Chemotherapy drugs	Types of NPs	Ref.
DOX	ZFH-DGR/DOX	163
	CAP/GA-sHA-DOX	168
	DOX/AL-azo/CH	169
	TLS11a-LB@TATp-MSN/DOX	170
	CAAP5G	171
PTX	DOX@Fe <sub>3</sub> O <sub>4</sub> -ZIF-8	172
	OPDEA-PCL	165
5-FU	Poly(allylamine)-based amphiphile	173
	Thiolated polymer-based nanocomposite	166
CDDP	NEM-5-FULPs	174
	Algal-mediated CuO	175
	CDDP/OA-LCC	176
ATO	ZrO <sub>2</sub>	177
	NGO-PEG-PEI	167

<sup>a</sup> ZFH-DGR: Zn<sup>2+</sup>-coordinated Fmoc His-Asp-Gly-Arg peptide; CAP: capsaicin; GA: glycyrrhetic acid; HA: hyaluronic acid; AL-azo: aligate-azo; CH: chitosan; TLS11a: HCC-specific aptamer; TATp: TAT peptide; CAAP5: cystamine dihydrochloride (CA)-capped pillar[5]arene; G: galactose derivative; OPDEA: poly[2-(N-oxide-*N,N*-diethylamino)ethyl methacrylate]; PCL: poly( $\epsilon$ -caprolactone); NEMs: nanoerythrocyte membranes; OA: oleanolic acid; LCC: lipid-coated calcium carbonate; PEI: polyethylenimine; Bcl-2, PI3K, Akt/PKB, and Stat-3 signaling pathways to inhibit HCC progression.<sup>188</sup> In addition, silver nanocolloid delivery of betulinic acid (BA) and polymeric micelles delivery of ursolic acid (UA) both increased the bioavailability of natural drugs.<sup>189,190</sup>

### 3.6 NPs for delivery of gene therapy

Gene therapy is a promising treatment for HCC, introducing exogenous genes to correct or improve tumor symptoms. It needs to be efficient, safe and specific.<sup>191</sup> RNAi is a promising gene silencing technology in HCC. The selective interaction between NPs and cellular molecules is a promising pathway for RNAi.<sup>192</sup> Extracellular vesicle (TDEV) membranes isolated from hepatocellular carcinoma cells were mixed into lipid nanovacuoles (LEVs) as small interfering RNA (siRNA) vectors, which have homing (into parental HCC cells) targeting ability and exponential transfection efficiency to enhance their anti-tumor ability by gene silencing at tumor loci.<sup>193</sup> The PEG- and GA-modified NGO adducts transporting siRNA have an effective VEGFa gene silencing effect.<sup>194</sup> Similarly, Wang *et al.* developed a novel biodegradable cationic polymer based on disulfide linkages loaded with small interfering VEGF RNA (siVEGF) with anti-HCC angiogenic effects.<sup>195</sup> Exosomes exogenously modified as microRNA (miRNA) carriers regulate the expression of their



downstream target genes to inhibit HCC cell proliferation and migration.<sup>196</sup> Furthermore, there are AuNPs, functionalized SeNPs, dipeptide NPs, *etc.* transporting different miRNAs to inhibit the corresponding downstream targets for HCC inhibition.<sup>197-199</sup>

### 3.7 NPs for immunotherapy

The use of immunotherapy in HCC has been a research point in recent years, where several immune checkpoint inhibitors such as Atezolizumab, Durvalumab and Nivolumab have been approved for use by the FDA, which activates the autoimmune system and allows immune cells to regain their killing power against tumor cells.<sup>200-202</sup> Qiang *et al.* formed chimeras by CNT/PEI and Durvalumab, which inhibited the expression of trigger receptor-2 on myeloid cells (Trem2), prolonged Durvalumab release, increased the proportion of T cells and CD8+ T cells, and promoted apoptosis in HCC cells compared to Durvalumab alone.<sup>203</sup> A novel nano-biomechanical probe was developed with which researchers tested the dissociation kinetics of three clinically approved PD-1 blocking monoclonal antibodies (Nivolumab, Pembrolizumab and Camrelizumab) and found a strong correlation between the three monoclonal antibodies and objective remission rates for HCC treatment, which could guide the screening, optimization and selection of therapeutic antibodies.<sup>204</sup>

Although the molecular mechanisms underlying chronic liver disease associated with HCC are unclear, factors associated with it, including a tumor-associated macrophage (TAM) and tumor microenvironment (TME), which are major factors as well as potential therapeutic targets.<sup>205</sup> A transferrin cell membrane nanovesicle encapsulated with IR820-dihydroartemisinin can activate oxidative stress to promote PD-L1-mediated immune checkpoint blockage (ICB), reshape the tumor immune microenvironment, and achieve dual T cell (CD4+ T and CD8+ T) activation, and IR820 molecules can also generate ROS under ultrasound activation to achieve multiple, precise anti-HCC effects.<sup>206</sup> In addition, a bicellular core-shell nanoparticle (TCN), TAM-based immunotherapy in conjunction with SRF, enhances m2-type TAM polarization for better synergistic anti-tumor effects.<sup>207</sup>

Moreover, an encapsulated ngc gel vaccine with tumor-specific neoantigens is used for the treatment and prevention of HCC. It activates an increase in 41BB+ CD8+ T cells, decreases the proportion of Foxp3+ CD25+ T cells, improves the intrahepatic immune microenvironment, and enhances the antitumor immune effect.<sup>208</sup>

## 4 Summary and outlook

HCC is a serious threat to human health as a malignant tumor of the digestive tract. Early diagnosis and effective treatment have been the focus of research. The advent of nanotechnology has brought promising modalities for the diagnosis and treatment of HCC. This paper summarizes the application of nanotechnology in these two aspects in recent years to provide further directions for future development. NPs have been

extensively studied for HCC imaging applications. NPs-based contrast imaging agents can be used at low concentrations to enhance the contrast and resolution in CT/PET and MRI imaging. In FMI imaging, especially intraoperative imaging, the results of the study showed more accurate and stable results than ICG, which is currently commonly used in clinical practice. In addition, NPs have shown significant results in multimodal imaging of HCC. NPs can sensitively detect AFP, GPC3 and CTCs at low limits in serological marker tests, which can be extremely helpful in the early diagnosis of HCC. In the treatment of HCC, NPs can not only kill HCC cells directly, but also act as chemotherapeutic agents, targeted drugs, gene therapy and immune carriers for targeted delivery to HCC cells. In addition, the improvement of embolic agents in TACE by nanotechnology can improve their efficacy. Not only that, NPs also treat HCC by PTT and PDT.

Although several NPs have been approved by the FDA for clinical use, the safety of NPs has always been an inevitable issue during their application in humans. The magnitude of their toxicity during retention in the body, the process of metabolism, and the rate of excretion need to be further studied and demonstrated. In most of the references, the effectiveness or activity of these materials is usually only studied, while the toxicological properties have not been fully studied and investigated, and only short-term animal experiments have proved to be relatively safe. While the toxicity of organic composite NPs is generally considered negligible, the long-term toxicity of these nanomaterials has never really been considered. In addition, based on the existing literature, nanomaterials are stored at room temperature for one week to one month, during which there will be no precipitation, dissolution or precipitation, *etc.*, so the formed NPs are considered to be relatively stable. In the literature, the efficacy of NPs after a period of time is not compromised. This is one of the reasons NPs have not entered clinical trials.

In conclusion, nanotechnology has a promising future in the diagnosis and treatment of HCC with great potential for improvement. For the early diagnosis of HCC, a combination of various methods (including imaging and serology, *etc.*) is needed to improve the diagnostic accuracy and lay the foundation for early treatment. In terms of treatment, multiple treatment modalities can be combined to reduce toxicity to normal hepatocytes, reduce drug resistance, and improve survival. Recently, the development of efficient diagnosis and treatment of integrated NPs is the direction of our efforts. The study of molecular mechanisms of NPs in HCC treatment may be the next step of effort.

## Author contributions

Conceptualization, W. J. and Y. Z.; writing – original draft preparation, W. J. and Y. H.; writing – review and editing, W. J., Y. H. and X. M.; suggestions on revision, W. X.; funding acquisition, Y. Z. All authors have read and agreed to the published version of the manuscript. All authors have contributed substantially to the work reported.



## Conflicts of interest

There are no conflicts to declare.

## Acknowledgements

This work was funded by the National Natural Science Foundation of China, grant number 81872255, 62041101, and the Key Medical Talents Foundation of Jiangsu Province, grant number 2016KJQWZDRC-03.

## References

- 1 A. Villanueva, *N. Engl. J. Med.*, 2019, **380**, 1450–1462.
- 2 J. Petrick, A. Florio, A. Znaor, D. Ruggieri, M. Laversanne, C. Alvarez, J. Ferlay, P. Valery, F. Bray and K. McGlynn, *Int. J. Cancer*, 2020, **147**, 317–330.
- 3 T. Akinyemiju, S. Abera, M. Ahmed, N. Alam, M. Alemayohu, C. Allen, R. Al-Raddadi, N. Alvis-Guzman, Y. Amoako, A. Artaman, T. Ayele, A. Barac, I. Bensenor, A. Berhane, Z. Bhutta, J. Castillo-Rivas, A. Chittheer, J. Choi, B. Cowie, L. Dandona, R. Dandona, S. Dey, D. Dicker, H. Phuc, D. Ekwueme, M. Zaki, F. Fischer, T. Fürst, J. Hancock, S. Hay, P. Hotez, S. Jee, A. Kasaeian, Y. Khader, Y. Khang, A. Kumar, M. Kutz, H. Larson, A. Lopez, R. Lunevicius, R. Malekzadeh, C. McAlinden, T. Meier, W. Mendoza, A. Mokdad, M. Moradi-Lakeh, G. Nagel, Q. Nguyen, G. Nguyen, F. Ogbo, G. Patton, D. Pereira, F. Pourmalek, M. Qorbani, A. Radfar, G. Rosenthal, J. Salomon, J. Sanabria, B. Sartorius, M. Satpathy, M. Sawhney, S. Sepanlou, K. Shackelford, H. Shore, J. Sun, D. Mengistu, R. Topór-Mądry, B. Tran, K. N. Ukwaja, V. Vlassov, S. Vollset, T. Vos, T. Wakayo, E. Weiderpass, A. Werdecker, N. Yonemoto, M. Younis, C. Yu, Z. Zaidi, L. Zhu, C. Murray, M. Naghavi and C. Fitzmaurice, *JAMA Oncol.*, 2017, **3**, 1683–1691.
- 4 F. Bray, J. Ferlay, I. Soerjomataram, R. Siegel, L. Torre and A. Jemal, *CA Cancer J. Clin.*, 2018, **68**, 394–424.
- 5 S. Mittal, J. Kramer, R. Omino, M. Chayanupatkul, P. Richardson, H. El-Serag and F. Kanwal, *Clin. Gastroenterol. Hepatol. Clin. Gastroenterol. Hepatol.*, 2018, **16**, 252–259.
- 6 F. Kanwal, J. Kramer, S. Asch, M. Chayanupatkul, Y. Cao and H. El-Serag, *Gastroenterology*, 2017, **153**, 996–1005.
- 7 K. McGlynn, J. Petrick and H. El-Serag, *Hepatology*, 2021, **4–13**, DOI: [10.1002/hep.31288](https://doi.org/10.1002/hep.31288).
- 8 H. El-Serag and F. Kanwal, *Hepatology*, 2014, **60**, 1767–1775.
- 9 C. Estes, H. Razavi, R. Loomba, Z. Younossi and A. Sanyal, *Hepatology*, 2018, **67**, 123–133.
- 10 N. Ganne-Carrié and P. Nahon, *J. Hepatol.*, 2019, **70**, 284–293.
- 11 F. Kanwal, J. Kramer, S. Mapakshi, Y. Natarajan, M. Chayanupatkul, P. Richardson, L. Li, R. Desiderio, A. Thrift, S. Asch, J. Chu and H. El-Serag, *Gastroenterology*, 2018, **155**, 1828–1837.
- 12 S. Katyal, J. Oliver, M. Peterson, J. Ferris, B. Carr and R. Baron, *Radiology*, 2000, **216**, 698–703.
- 13 M. Natsuzaka, T. Omura, T. Akaike, Y. Kuwata, K. Yamazaki, T. Sato, Y. Karino, J. Toyota, T. Suga and M. Asaka, *J. Gastroenterol. Hepatol.*, 2005, **20**, 1781–1787.
- 14 M. Le Grazie, M. Biagini, M. Tarocchi, S. Polvani and A. Galli, *World J. Hepatol.*, 2017, **9**, 907–920.
- 15 A. Benson, M. D'Angelica, D. Abbott, D. Anaya, R. Anders, C. Are, M. Bachini, M. Borad, D. Brown, A. Burgoyne, P. Chahal, D. Chang, J. Cloyd, A. Covey, E. Glazer, L. Goyal, W. Hawkins, R. Iyer, R. Jacob, R. Kelley, R. Kim, M. Levine, M. Palta, J. Park, S. Raman, S. Reddy, V. Sahai, T. Schefter, G. Singh, S. Stein, J. Vauthhey, A. Venook, A. Yopp, N. McMillian, C. Hochstetler and S. Darlow, *J. Natl. Compr. Cancer Netw.*, 2021, **19**, 541–565.
- 16 K. Schulze, S. Imbeaud, E. Letouzé, L. Alexandrov, J. Calderaro, S. Rebouissou, G. Couchy, C. Meiller, J. Shinde, F. Soysouvanh, A. Calatayud, R. Pinyol, L. Pelletier, C. Balabaud, A. Laurent, J. Blanc, V. Mazzaferro, F. Calvo, A. Villanueva, J. Nault, P. Bioulac-Sage, M. Stratton, J. Llovet and J. Zucman-Rossi, *Nat. Genet.*, 2015, **47**, 505–511.
- 17 D. Galun, D. Mijac, A. Filipovic, A. Bogdanovic, M. Zivanovic and D. Masulovic, *J. Pers. Med.*, 2022, **12**.
- 18 J. Zucman-Rossi, A. Villanueva, J. Nault and J. Llovet, *Gastroenterology*, 2015, **149**, 1226–1239.
- 19 S. Zhang, Q. Li, N. Yang, Y. Shi and X. Dong, *Adv. Funct. Mater.*, 2019, **29**, 190685.1–190685.9.
- 20 S. Zhang, C. Cao, X. Lv, H. Dai, Z. Zhong, C. Liang, W. Wang, W. Huang, X. Song and X. Dong, *Chem. Sci.*, 2020, **11**, 1926–1934.
- 21 D. Chen, Q. Tang, J. Zou, X. Yang, W. Huang, Q. Zhang, J. Shao and X. Dong, *Adv. Healthcare Mater.*, 2018, **7**, e1701272.
- 22 S. Mohamed, S. Veeranarayanan, T. Maekawa and D. Sakthi Kumar, *Adv. Drug Deliv. Rev.*, 2019, **138**, 18–40.
- 23 F. Danhier, *J. Controlled Release*, 2016, **244**, 108–121.
- 24 Y. Cai, Q. Tang, X. Wu, W. Si, Q. Zhang, W. Huang and X. Dong, *ACS Appl. Mater. Interfaces*, 2016, **8**, 10737–10742.
- 25 R. Petros and J. DeSimone, *Nat. Rev. Drug Discov.*, 2010, **9**, 615–627.
- 26 H. Makadia and S. Siegel, *Polymers*, 2011, **3**, 1377–1397.
- 27 S. Rezvantalab, N. Drude, M. Moraveji, N. Güvener, E. Koons, Y. Shi, T. Lammers and F. Kiessling, *Front. Pharmacol.*, 2018, **9**, 1260.
- 28 J. Kim, G. Hong, L. Mazaleuskaya, J. Hsu, D. Rosario-Berrios, T. Grosser, P. Cho-Park and D. Cormode, *ACS Appl. Mater. Interfaces*, 2021, **13**, 60852–60864.
- 29 S. Ning, Y. Zheng, K. Qiao, G. Li, Q. Bai and S. Xu, *J. Nanobiotechnol.*, 2021, **19**, 344.
- 30 A. Alhalmi, S. Beg, K. Kohli, M. Waris and T. Singh, *Curr. Drug Targets*, 2021, **22**, 779–792.
- 31 F. Graur, A. Puia, E. I. Mois, S. Moldovan, A. Pusta, C. Cristea, S. Cavalu, C. Puia and N. Al Hajjar, *Materials*, 2022, **15**, 3893.
- 32 Q. Tang, W. Si, C. Huang, K. Ding, W. Huang, P. Chen, Q. Zhang and X. Dong, *J. Mater. Chem. B*, 2017, **5**, 1566–1573.



33 W. Xiao, P. Wang, C. Ou, X. Huang, Y. Tang, M. Wu, W. Si, J. Shao, W. Huang and X. Dong, *Biomaterials*, 2018, **183**, 1–9.

34 Y. Wang, X. Huang, Y. Tang, J. Zou, P. Wang, Y. Zhang, W. Si, W. Huang and X. Dong, *Chem. Sci.*, 2018, **9**, 8103–8109.

35 G. Liu, S. Zhang, Y. Shi, X. Huang, Y. Tang, P. Chen, W. Si, W. Huang and X. Dong, *Adv. Funct. Mater.*, 2018, **28**, 1804317.1–1804317.11.

36 C. Chang, H. Chen, Y. Chang, M. Yang, C. Lo, W. Ko, Y. Lee, K. Liu and R. Chang, *Comput. Methods Programs Biomed.*, 2017, **145**, 45–51.

37 European Association for Study of Liver and European Organisation for Research and Treatment of Cancer, European Association for Study of Liver; European Organisation for Research and Treatment of Cancer. EASL-EORTC clinical practice guidelines: management of hepatocellular carcinoma, *Eur. J. Cancer*, 2012, **48**(5), 599–641; *Erratum in: Eur. J. Cancer*, 2012, **48**(8), 1255–1256, PMID: 22424278.

38 O. Matsui, S. Kobayashi, J. Sanada, W. Kouda, Y. Ryu, K. Kozaka, A. Kitao, K. Nakamura and T. Gabata, *Abdom. Imaging*, 2011, **36**, 264–272.

39 L. Roberts, C. Sirlin, F. Zaiem, J. Almasri, L. Prokop, J. Heimbach, M. Murad and K. Mohammed, *Hepatology*, 2018, **67**, 401–421.

40 L. Xiang, N. Anton, G. Zuber and T. Vandamme, *Adv. Drug Deliv. Rev.*, 2014, **76**, 116–133.

41 S. T. Schindera, L. F. Hareter, S. Raible, J. C. Torrente and Z. Szucs-Farkas, *Invest. Radiol.*, 2012, **47**, 197–201.

42 K. Dongkyu, P. Sangjin, J. H. Lee and Y. Y. Jeong, *J. Am. Chem. Soc.*, 2007, **129**, 12585.

43 D. Rand, V. Ortiz, Y. Liu, Z. Derdak, J. Wands, M. Tatićek and C. Rose-Petrucci, *Nano Lett.*, 2011, **11**, 2678–2683.

44 S. Prajapati and C. Keller, *J. Vis. Exp.*, 2011, **27**, 2377.

45 J. Rothe, I. Rudolph, N. Rohwer, D. Kupitz, B. Gregor-Mamoudou, T. Derlin, C. Furth, H. Amthauer, W. Brenner, R. Buchert, T. Cramer and I. Apostolova, *Acad. Radiol.*, 2015, **22**, 169–178.

46 N. Anton, A. Parlog, G. B. About, M. F. Attia, M. Wattenhofer-Donzé, H. Jacobs, I. Goncalves, E. Robinet, T. Sorg and T. F. Vandamme, *Sci. Rep.*, 2017, **7**, 13935.

47 H. Ni, C. Yu, S. Chen, L. Chen, C. Lin, W. Lee, C. Chuang, C. Ho, C. Chang and T. Lee, *Appl. Radiat. Isot.*, 2015, **99**, 117–121.

48 B. Ariff, C. Lloyd, S. Khan, M. Shariff, A. Thillainayagam, D. Bansi, S. Khan, S. Taylor-Robinson and A. Lim, *World J. Gastroenterol.*, 2009, **15**, 1289–1300.

49 B. Howard and T. Wong, *Radiol. Clin. North Am.*, 2021, **59**, 737–753.

50 S. Kwee, M. Tiirikainen, M. Sato, J. Acoba, R. Wei, W. Jia, L. Le Marchand and L. Wong, *Cancer Res.*, 2019, **79**, 1696–1704.

51 M. Silindir, A. Özer and S. Erdogan, *Drug. Deliv.*, 2012, **19**, 68–80.

52 A. Karaosmanoglu, M. Onur, M. Ozmen, D. Akata and M. Karcaaltincaba, *Semin. Ultrasound CT MRI*, 2016, **37**, 533–548.

53 Z. Chen, D. Yu, S. Wang, N. Zhang, C. Ma and Z. Lu, *Nanoscale Res. Lett.*, 2009, **4**, 618–626.

54 S. Geninatti Crich, J. Cutrin, S. Lanzardo, L. Conti, F. Kálmán, I. Szabó, N. Lago, A. Iolascon and S. Aime, *Contrast Media Mol. Imaging*, 2012, **7**, 281–288.

55 W. Hou, T. B. Toh, L. N. Abdullah, T. Yvonne, K. J. Lee, I. Guenther and K. H. Chow, *Nanomed.: Nanotechnol. Biol. Med.*, 2017, **13**, 783–793.

56 R. Hachani, M. A. Birchall, M. W. Lowdell, G. Kasparis, L. D. Tung, B. B. Manshian, S. J. Soenen, W. Gsell, U. Himmelreich and C. A. Gharagouzloo, *Sci. Rep.*, 2017, **7**, 7850.

57 R. Khatik, Z. Wang, F. Li, D. Zhi, S. Kiran, P. Dwivedi, R. Xu, G. Liang, B. Qiu and Q. Yang, *Nanomed.: Nanotechnol. Biol. Med.*, 2019, **15**, 264–273.

58 D. Aufhauser, E. Sadot, D. Murken, K. Eddinger, M. Hoteit, P. Abt, D. Goldberg, R. DeMatteo and M. Levine, *Ann. Surg.*, 2018, **267**, 922–928.

59 A. Antaris, H. Chen, K. Cheng, Y. Sun, G. Hong, C. Qu, S. Diao, Z. Deng, X. Hu, B. Zhang, X. Zhang, O. Yaghi, Z. Alamparambil, X. Hong, Z. Cheng and H. Dai, *Nat. Mater.*, 2016, **15**, 235–242.

60 Q. Nguyen, E. Olson, T. Aguilera, T. Jiang, M. Scadeng, L. Ellies and R. Tsien, *Proc. Natl. Acad. Sci. U. S. A.*, 2010, **107**, 4317–4322.

61 K. Mori, H. Ohishi, M. Yamamoto, T. Yamamoto and Y. Nakao, *Innov. Neurosurg.*, 2013, **1**, 109–113.

62 T. Tanaka, M. Takatsuki, M. Hidaka, T. Hara, I. Muraoka, A. Soyama, T. Adachi, T. Kuroki and S. Eguchi, *J. Hepatobiliary Pancreat. Sci.*, 2014, **21**, 199–204.

63 K. Gotoh, T. Yamada, O. Ishikawa, H. Takahashi, H. Eguchi, M. Yano, H. Ohigashi, Y. Tomita, Y. Miyamoto and S. Imaoka, *J. Surg. Oncol.*, 2009, **100**, 75–79.

64 Y. Dai, L. Zhu, Y. Zhang, S. Wang, K. Chen, T. Jiang, X. Xu and X. Geng, *Hepatobiliary Pancreatic Dis. Int.*, 2019, **18**, 266–272.

65 Z. Hu, C. Chi, M. Liu, H. Guo, Z. Zhang, C. Zeng, J. Ye, J. Wang, J. Tian, W. Yang and W. Xu, *Nanomed.: Nanotechnol. Biol. Med.*, 2017, **13**, 1323–1331.

66 Q. Duan, M. Che, S. Hu, H. Zhao, Y. Li, X. Ma, W. Zhang, Y. Zhang and S. Sang, *Anal. Bioanal. Chem.*, 2019, **411**, 967–972.

67 S. Mukherjee and F. Maxfield, *Annu. Rev. Cell Dev. Biol.*, 2004, **20**, 839–866.

68 Z. Li, J. Cheng, P. Huang, W. Song, L. Nong, L. Huang and W. Lin, *Anal. Chem.*, 2022, **94**, 3386–3393.

69 C. Andreou, V. Neuschmelting, D. Tschaharganeh, C. Huang, A. Oseledchyk, P. Iacono, H. Karabeber, R. Colen, L. Mannelli, S. Lowe and M. Kircher, *ACS Nano*, 2016, **10**, 5015–5026.

70 C. Sciallero, L. Balbi, G. Paradossi and A. Trucco, *R. Soc. Open Sci.*, 2016, **3**, 160063.

71 P. Yang, F. Wang, X. Luo, Y. Zhang, J. Guo, W. Shi and C. Wang, *ACS Appl. Mater. Interfaces*, 2014, **6**, 12581–12587.



72 H. Guo, Z. Jiang, S. Song, T. Dai, X. Wang, K. Sun, G. Zhou and H. Dou, *J. Colloid Interface Sci.*, 2016, **482**, 95–104.

73 F. Maghsoudinia, M. Tavakoli, R. Samani, S. Hejazi, T. Sobhani, F. Mehradnia and M. Mehrgardi, *Talanta*, 2021, **228**, 122245.

74 Y. Jin, K. Wang and J. Tian, *Bioconjugate Chem.*, 2018, **29**, 1475–1484.

75 Y. Ren, S. He, L. Huttad, M. Chua, S. So, Q. Guo and Z. Cheng, *Nanoscale*, 2020, **12**, 11510–11517.

76 H. Zhang, L. Deng, H. Liu, S. Mai, Z. Cheng, G. Shi, H. Zeng and Z. Wu, *Mater. Today Bio*, 2022, **13**, 100220.

77 P. Lei, H. Chen, C. Feng, X. Yuan, Z. Xiong, Y. Liu and W. Liao, *ACS Nano*, 2022, **16**, 897–909.

78 M. Serper, T. Taddei, R. Mehta, K. D'Addeo, F. Dai, A. Aytaman, M. Baytarian, R. Fox, K. Hunt, D. Goldberg, A. Valderrama and D. Kaplan, *Gastroenterology*, 2017, **152**, 1954–1964.

79 S. Berhane, H. Toyoda, T. Tada, T. Kumada, C. Kagebayashi, S. Satomura, N. Schweitzer, A. Vogel, M. Manns, J. Benckert, T. Berg, M. Ebker, J. Best, A. Dechêne, G. Gerken, J. Schlaak, A. Weinmann, M. Wörns, P. Galle, W. Yeo, F. Mo, S. Chan, H. Reeves, T. Cox and P. Johnson, *Clin. Gastroenterol. Hepatol. Clin. Gastroenterol. Hepatol.*, 2016, **14**, 875–886.

80 M. Reig, A. Forner, J. Rimola, J. Ferrer-Fàbrega, M. Burrel, Á. Garcia-Criado, R. Kelley, P. Galle, V. Mazzaferro, R. Salem, B. Sangro, A. Singal, A. Vogel, J. Fuster, C. Ayuso and J. Bruix, *J. Hepatol.*, 2022, **76**, 681–693.

81 Z. Luo, L. Zhang, R. Zeng, L. Su and D. Tang, *Anal. Chem.*, 2018, **90**, 9568–9575.

82 D. Sun, H. Li, M. Li, C. Li, L. Qian and B. Yang, *Biosens. Bioelectron.*, 2019, **132**, 68–75.

83 X. Ran, R. Yuan, Y. Chai, C. Hong and X. Qian, *Colloids Surf., B*, 2010, **79**, 421–426.

84 Q. Zhu, R. Yuan, Y. Chai, J. Han, Y. Li and N. Liao, *Analyst*, 2013, **138**, 620–626.

85 J. Rashidiani, M. Kamali, H. Sedighian, M. Akbariqomi, M. Mansouri and H. Kooshki, *Biosens. Bioelectron.*, 2018, **102**, 226–233.

86 Y. Cao, R. Yuan, Y. Chai, L. Mao, H. Niu, H. Liu and Y. Zhuo, *Biosens. Bioelectron.*, 2012, **31**, 305–309.

87 G. Jie, J. Zhang, D. Wang, C. Cheng, H. Chen and J. Zhu, *Anal. Chem.*, 2008, **80**, 4033–4039.

88 Y. Ding, J. Liu, H. Wang, G. Shen and R. Yu, *Biomaterials*, 2007, **28**, 2147–2154.

89 H. Zhou, N. Gan, T. Li, Y. Cao, S. Zeng, L. Zheng and Z. Guo, *Anal. Chim. Acta*, 2012, **746**, 107–113.

90 H. Xu, D. Wang, S. He, J. Li, B. Feng, P. Ma, P. Xu, S. Gao, S. Zhang, Q. Liu, J. Lu, S. Song and C. Fan, *Biosens. Bioelectron.*, 2013, **50**, 251–255.

91 S. Yuan, R. Yuan, Y. Chai, L. Mao, X. Yang, Y. Yuan and H. Niu, *Talanta*, 2010, **82**, 1468–1471.

92 H. Su, R. Yuan, Y. Chai, L. Mao and Y. Zhuo, *Biosens. Bioelectron.*, 2011, **26**, 4601–4604.

93 W. Li, X. Jiang, J. Xue, Z. Zhou and J. Zhou, *Biosens. Bioelectron.*, 2015, **68**, 468–474.

94 Y. Wei, Y. Li, N. Li, Y. Zhang, T. Yan, H. Ma and Q. Wei, *Biosens. Bioelectron.*, 2016, **79**, 482–487.

95 Y. Wu, W. Guo, W. Peng, Q. Zhao, J. Piao, B. Zhang, X. Wu, H. Wang, X. Gong and J. Chang, *ACS Appl. Mater. Interfaces*, 2017, **9**, 9369–9377.

96 L. Yu, Q. Zhang, Q. Kang, B. Zhang, D. Shen and G. Zou, *Anal. Chem.*, 2020, **92**, 7581–7587.

97 N. Jo and Y. Shin, *Sci. Rep.*, 2020, **10**, 1024.

98 N. Jo, K. Lee and Y. Shin, *Biosens. Bioelectron.*, 2016, **81**, 324–333.

99 X. Zhong, M. Zhang, L. Guo, Y. Xie, R. Luo, W. Chen, F. Cheng and L. Wang, *Biosens. Bioelectron.*, 2021, **189**, 113389.

100 X. Wang, J. Ji, P. Yang, X. Li, Y. Pang and P. Lu, *Talanta*, 2022, **243**, 123328.

101 J. Guo, S. Li, J. Wang and J. Wang, *Biosens. Bioelectron.*, 2022, **198**, 113820.

102 H. Yu, X. Tan, S. Sun, L. Zhang, C. Gao and S. Ge, *Biosens. Bioelectron.*, 2021, **185**, 113250.

103 B. Zhao, J. Yan, D. Wang, Z. Ge, S. He, D. He, S. Song and C. Fan, *Small*, 2013, **9**, 2595–2601.

104 C. Wang, F. Hou and Y. Ma, *Biosens. Bioelectron.*, 2015, **68**, 156–162.

105 L. Zhou, J. Zhou, Z. Feng, F. Wang, S. Xie and S. Bu, *Analyst*, 2016, **141**, 2534–2541.

106 Q. Wu, F. Zhang, H. Li, Z. Li, Q. Kang and D. Shen, *Analyst*, 2018, **143**, 5030–5037.

107 L. Chen, X. Wang, Q. Zhang, Z. Li, Q. Kang and D. Shen, *Analyst*, 2020, **145**, 2389–2397.

108 X. Li, X. Pan, J. Lu, Y. Zhou and J. Gong, *Biosens. Bioelectron.*, 2020, **158**, 112158.

109 Y. Wu, H. Liu and H. Ding, *J. Hepatocell. Carcinoma*, 2016, **3**, 63–67.

110 W. Mu, D. Jiang, S. Mu, S. Liang, Y. Liu and N. Zhang, *ACS Appl. Mater. Interfaces*, 2019, **11**, 23591–23604.

111 S. Zhao, M. Long, X. Zhang, S. Lei, W. Dou, J. Hu, X. Du and L. Liu, *Ann. Transl. Med.*, 2020, **8**, 536.

112 S. Yu, Z. Li, J. Li, S. Zhao, S. Wu, H. Liu, X. Bi, D. Li, J. Dong, S. Duan and B. Hammock, *Sens. Actuators, B*, 2021, 336.

113 Y. Huang, H. Li, T. Gao, X. Liu and G. Li, *Analyst*, 2014, **139**, 3744–3747.

114 T. Tayoun, V. Faugeroux, M. Oulhen, A. Aberlenc, P. Pawlikowska and F. Farace, *Cells*, 2019, **8**, 1145.

115 L. Qi, B. Xiang, F. Wu, J. Ye, J. Zhong, Y. Wang, Y. Chen, Z. Chen, L. Ma, J. Chen, W. Gong, Z. Han, Y. Lu, J. Shang and L. Li, *Cancer Res.*, 2018, **78**, 4731–4744.

116 R. Kelley, M. Magbanua, T. Butler, E. Collisson, J. Hwang, N. Sidiropoulos, K. Eason, R. McWhirter, B. Hameed, E. Wayne, F. Yao, A. Venook and J. Park, *BMC Cancer*, 2015, **15**, 206.

117 W. Xia, H. Li, Y. Li, M. Li, J. Fan, W. Sun, N. Li, R. Li, K. Shao and X. Peng, *Nano Lett.*, 2021, **21**, 634–641.

118 W. Xie, T. Yin, Y. Chen, D. Zhu, M. Zan, B. Chen, L. Ji, L. Chen, S. Guo, H. Huang, X. Zhao, Y. Wang, Y. Wu and W. Liu, *Nanoscale*, 2019, **11**, 8293–8303.

119 C. Wu, P. Li, N. Fan, J. Han, W. Zhang, W. Zhang and B. Tang, *ACS Appl. Mater. Interfaces*, 2019, **11**, 44999–45006.

120 J. Llovet, A. Villanueva, J. Marrero, M. Schwartz, T. Meyer, P. Galle, R. Lencioni, T. Greten, M. Kudo, S. Mandrekar,



A. Zhu, R. Finn and L. Roberts, *Hepatology*, 2021, 158–191, DOI: [10.1002/hep.31327](https://doi.org/10.1002/hep.31327).

121 J. Llovet, C. Brú and J. Bruix, *Semin. Liver Dis.*, 1999, **19**, 329–338.

122 G. D'Amico, A. Morabito, M. D'Amico, L. Pasta, G. Malizia, P. Rebora and M. Valsecchi, *J. Hepatol.*, 2018, **68**, 563–576.

123 J. Llovet, J. Bustamante, A. Castells, R. Vilana, M. C. Ayuso, M. Sala, C. Brú, J. Rodés and J. Bruix, *Hepatology*, 1999, **29**, 62–67.

124 O. Miltiadous, D. Sia, Y. Hoshida, M. Fiel, A. Harrington, S. Thung, P. Tan, H. Dong, K. Revill, C. Chang, S. Roayaie, T. Byrne, V. Mazzaferro, J. Rakela, S. Florman, M. Schwartz and J. Llovet, *J. Hepatol.*, 2015, **63**, 1368–1377.

125 J. Llovet, T. De Baere, L. Kulik, P. Haber, T. Greten, T. Meyer and R. Lencioni, *Nat. Rev. Gastroenterol. Hepatol.*, 2021, **18**, 293–313.

126 Y. Shao, B. Arjun, H. Leo and K. Chua, *J. Therm. Biol.*, 2017, **66**, 101–113.

127 A. Ashokan, V. Somasundaram, G. Gowd, I. Anna, G. Malarvizhi, B. Sridharan, R. Jobanputra, R. Peethambaran, A. Unni, S. Nair and M. Koyakutty, *Sci. Rep.*, 2017, **7**, 14481.

128 L. Liu, Z. Xiao, Y. Xiao, Z. Wang, F. Li, M. Li and X. Peng, *Oncol. Lett.*, 2014, **7**, 1485–1492.

129 H. Hu, G. Chen, W. Yuan, J. Wang and B. Zhai, *Int. J. Hyperthermia*, 2018, **34**, 1351–1358.

130 Q. Zhou, N. Gong, D. Zhang, J. Li, X. Han, J. Dou, J. Huang, K. Zhu, P. Liang, X. Liang and J. Yu, *ACS Nano*, 2021, **15**, 2920–2932.

131 J. Li and K. Pu, *Acc. Chem. Res.*, 2020, **53**, 752–762.

132 X. Chen, Q. Zhang, J. Li, M. Yang, N. Zhao and F. Xu, *ACS Nano*, 2018, **12**, 5646–5656.

133 L. Mocan, C. Matea, F. Tabaran, O. Mosteanu, T. Pop, C. Puia, L. Agoston-Coldea, G. Zaharie, T. Mocan, A. Buzoianu and C. Iancu, *Biomaterials*, 2017, **119**, 33–42.

134 C. Xu, D. Yang, L. Mei, Q. Li, H. Zhu and T. Wang, *ACS Appl. Mater. Interfaces*, 2013, **5**, 12911–12920.

135 C. Wen, R. Cheng, T. Gong, Y. Huang, D. Li, X. Zhao, B. Yu, D. Su, Z. Song and W. Liang, *Colloids Surf., B*, 2021, **199**, 111510.

136 B. Ji, H. Cai, Y. Yang, F. Peng, M. Song, K. Sun, F. Yan and Y. Liu, *Acta Biomater.*, 2020, **111**, 363–372.

137 A. Oniszczuk, K. Wojtunik-Kulesza, T. Oniszczuk and K. Kasprzak, *Biomed. Pharmacother.*, 2016, **83**, 912–929.

138 D. Hu, L. Chen, Y. Qu, J. Peng, B. Chu, K. Shi, Y. Hao, L. Zhong, M. Wang and Z. Qian, *Theranostics*, 2018, **8**, 1558–1574.

139 Y. Han, Y. An, G. Jia, X. Wang, C. He, Y. Ding and Q. Tang, *Nanoscale*, 2018, **10**, 6511–6523.

140 J. Kaneko, T. Kokudo, Y. Inagaki and K. Hasegawa, *Transl. Gastroenterol. Hepatol.*, 2018, **3**, 78.

141 M. Lan, S. Zhao, W. Liu, C. Lee, W. Zhang and P. Wang, *Adv. Healthcare Mater.*, 2019, **8**, e1900132.

142 J. Kim, C. Tung and Y. Choi, *Chem. Commun.*, 2014, **50**, 10600–10603.

143 H. Kang, S. Rho, W. Stiles, S. Hu, Y. Baek, D. Hwang, S. Kashiwagi, M. Kim and H. Choi, *Adv. Healthcare Mater.*, 2020, **9**, e1901223.

144 D. Abdel Fadool, G. Al-Toukhy, A. Elsharif, S. Al-Jameel, H. Mohamed and T. Youssef, *Photodiagnosis Photodyn Ther.*, 2018, **23**, 25–31.

145 J. Xu, Q. Zheng, X. Cheng, S. Hu, C. Zhang, X. Zhou, P. Sun, W. Wang, Z. Su, T. Zou, Z. Song, Y. Xia, X. Yi and Y. Gao, *J. Nanobiotechnol.*, 2021, **19**, 355.

146 J. Kwon, I. Song, M. Kim, B. Lee, J. Kim, I. Yoon, Y. Shim, N. Kim, J. Han and J. Youm, *Integr. Med. Res.*, 2013, **2**, 106–111.

147 Z. Feng, J. Guo, X. Liu, H. Song, C. Zhang, P. Huang, A. Dong, D. Kong and W. Wang, *Biomaterials*, 2020, **255**, 120210.

148 A. Facciorusso, *World J. Gastroenterol.*, 2018, **24**, 161–169.

149 F. Piscaglia and S. Ogasawara, *Liver Cancer*, 2018, **7**, 104–119.

150 S. Daher, M. Massarwa, A. Benson and T. Khoury, *J. Clin. Transl. Hepatol.*, 2018, **6**, 69–78.

151 D. Kong, T. Jiang, J. Liu, X. Jiang, B. Liu, C. Lou, B. Zhao, S. Carroll and G. Feng, *Drug. Deliv.*, 2020, **27**, 1729–1740.

152 L. Wei-Ze, H. Wen-Xia, Z. Ning, H. Shu-Miao, L. Fei, F. Li-Na, Z. Zhan-Rui, Z. Xi-Feng and Y. Li-Bin, *Eur. J. Pharm. Sci.*, 2020, **153**, 105496.

153 Y. Wang, W. Shang, H. Zhong, T. Luo, M. Niu, K. Xu and J. Tian, *ACS Nano*, 2020, **14**, 14907–14918.

154 A. Dev, A. Sood, S. Choudhury and S. Karmakar, *Mater. Sci. Eng., C*, 2020, **107**, 110315.

155 D. Su, *Bioengineered*, 2021, **12**, 11124–11135.

156 D. Wang, Q. Wu, R. Guo, C. Lu, M. Niu and W. Rao, *Nanoscale*, 2021, **13**, 8817–8836.

157 H. Ahmed, W. Khalil and A. Hamza, *Toxicol. Mech. Methods*, 2014, **24**, 593–602.

158 B. Zhu, Y. Li, Z. Lin, M. Zhao, T. Xu, C. Wang and N. Deng, *Nanoscale Res. Lett.*, 2016, **11**, 198.

159 K. Kitchin, J. Richards, B. Robinette, K. Wallace, N. Coates, B. Castellon, E. Grulke, J. Kou and R. Varma, *J. Nanosci. Nanotechnol.*, 2020, **20**, 5833–5858.

160 L. Liu, H. Dai, Y. Wu, B. Li, J. Yi, C. Xu and X. Wu, *Int. J. Nanomed.*, 2019, **14**, 3491–3502.

161 Y. Niu, E. Tang and Q. Zhang, *Toxicol. Res.*, 2019, **8**, 1042–1049.

162 M. Younas, M. Rizwan, M. Zubair, A. Inam and S. Ali, *Ecotoxicol. Environ. Saf.*, 2021, **223**, 112575.

163 B. Mugaka, S. Zhang, R. Li, Y. Ma, B. Wang, J. Hong, Y. Hu, Y. Ding and X. Xia, *ACS Appl. Mater. Interfaces*, 2021, **13**, 11195–11204.

164 A. Usmani, A. Mishra, M. Arshad and A. Jafri, *Artif. Cells, Nanomed., Biotechnol.*, 2019, **47**, 933–944.

165 W. Fan, Q. Wei, J. Xiang, Y. Tang, Q. Zhou, Y. Geng, Y. Liu, R. Sun, L. Xu, G. Wang, Y. Piao, S. Shao, Z. Zhou, J. Tang, T. Xie, Z. Li and Y. Shen, *Adv. Mater.*, 2022, **34**, e2109189.

166 S. Bhat, D. Mukherjee, P. Sukharamwala, R. Dehuri, A. Murali and B. Teja, *Drug Deliv. Transl. Res.*, 2021, **11**, 2252–2269.



167 S. Wang, Y. Ma, X. Chen, Y. Zhao and X. Mou, *Front. Pharmacol.*, 2019, **10**, 69.

168 Z. Li, F. Wang, Y. Li, X. Wang, Q. Lu, D. Wang, C. Qi, C. Li, Z. Li, B. Lian, G. Tian, Z. Gao, B. Zhang and J. Wu, *Biomaterials*, 2021, **276**, 121003.

169 Q. Chen, X. Li, Y. Xie, W. Hu, Z. Cheng, H. Zhong and H. Zhu, *Int. J. Biol. Macromol.*, 2021, **187**, 214–222.

170 Z. Ding, D. Wang, W. Shi, X. Yang, S. Duan, F. Mo, X. Hou, A. Liu and X. Lu, *Int. J. Nanomed.*, 2020, **15**, 8383–8400.

171 Y. Lu, C. Hou, J. Ren, K. Yang, Y. Chang, Y. Pei, H. Dong and Z. Pei, *Int. J. Nanomed.*, 2019, **14**, 3525–3532.

172 C. Cheng, C. Li, X. Zhu, W. Han, J. Li and Y. Lv, *J. Biomater. Appl.*, 2019, **33**, 1373–1381.

173 W. Al-Shakarchi, A. Alsuraiifi, A. Curtis and C. Hoskins, *Pharmaceutics*, 2018, **10**.

174 S. AlQahtani, G. Harisa, M. Badran, K. AlGhamdi, A. Kumar, M. Salem-Bekhit, S. Ahmad and F. Alanazi, *Artif. Cells, Nanomed., Biotechnol.*, 2019, **47**, 989–996.

175 N. Aboeita, S. Fahmy, M. El-Sayed, H. Azzazy and T. Shoeib, *Pharmaceutics*, 2022, **14**.

176 M. Khan, P. Zhao, A. Khan, F. Raza, S. Raza, M. Sarfraz, Y. Chen, M. Li, T. Yang, X. Ma and G. Xiang, *Int. J. Nanomed.*, 2019, **14**, 3753–3771.

177 Q. Wu, X. Chen, P. Wang, Q. Wu, X. Qi, X. Han, L. Chen, X. Meng and K. Xu, *ACS Appl. Mater. Interfaces*, 2020, **12**, 8016–8029.

178 Y. Sun, W. Ma, Y. Yang, M. He, A. Li, L. Bai, B. Yu and Z. Yu, *Asian J. Pharm. Sci.*, 2019, **14**, 581–594.

179 J. Llovet, R. Montal, D. Sia and R. Finn, *Nat. Rev. Clin. Oncol.*, 2018, **15**, 599–616.

180 J. Kaur, S. Tuler and C. Dasanu, *J. Oncol. Pharm. Pract.*, 2022, **28**, 475–478.

181 L. Ding, P. Zhang, X. Huang, K. Yang, X. Liu and Z. Yu, *Front. Pharmacol.*, 2021, **12**, 809125.

182 B. Wang, L. Sun, M. Wen, Y. Tan, W. Almalki, H. Katouah, I. Kazmi, O. Afzal, A. Altamimi, F. Al-Abbas, M. Alrobaian, K. Alharbi, S. Alenezi, A. Alghaith, S. Beg and M. Rahman, *Saudi Pharm. J.*, 2021, **29**, 843–856.

183 H. Tang, C. Li, Y. Zhang, H. Zheng, Y. Cheng, J. Zhu, X. Chen, Z. Zhu, J. Piao and F. Li, *Theranostics*, 2020, **10**, 9865–9887.

184 L. Tunki, H. Kulhari, L. Vadithe, M. Kuncha, S. Bhargava, D. Pooja and R. Sistla, *Eur. J. Pharm. Sci.*, 2019, **137**, 104978.

185 D. Ling, H. Xia, W. Park, M. Hackett, C. Song, K. Na, K. Hui and T. Hyeon, *ACS Nano*, 2014, **8**, 8027–8039.

186 H. Abbas, Y. El-Feky, M. Al-Sawahli, N. El-Deeb, H. El-Nassan and M. Zewail, *Drug. Deliv.*, 2022, **29**, 714–727.

187 S. Kianamiri, A. Dinari, M. Sadeghizadeh, M. Rezaei, B. Daraei, N. Bahsoun and A. Noman, *Mol. Pharmaceutics*, 2020, **17**, 4483–4498.

188 M. Rahman, S. Al-Ghamdi, K. Alharbi, S. Beg, K. Sharma, F. Anwar, F. Al-Abbas and V. Kumar, *Drug. Deliv.*, 2019, **26**, 782–793.

189 M. Zhou, Y. Yi, L. Liu, Y. Lin, J. Li, J. Ruan and Z. Zhong, *J. Cancer*, 2019, **10**, 5820–5831.

190 I. Pinzaru, C. Sarau, D. Coricovac, I. Marcovici, C. Utescu, S. Tofan, R. Popovici, H. Manea, I. Pavel, C. Soica and C. Dehelean, *Nanomaterials*, 2021, **11**, 152.

191 T. Li, G. Kang, T. Wang and H. Huang, *Oncol. Lett.*, 2018, **16**, 687–702.

192 S. Senapati, T. Sarkar, P. Das and P. Maiti, *Bioconjugate Chem.*, 2019, **30**, 2544–2554.

193 X. Zhou, Y. Miao, Y. Wang, S. He, L. Guo, J. Mao, M. Chen, Y. Yang, X. Zhang and Y. Gan, *J. Extracell. Vesicles*, 2022, **11**, e12198.

194 Y. Qu, F. Sun, F. He, C. Yu, J. Lv, Q. Zhang, D. Liang, C. Yu, J. Wang, X. Zhang, A. Xu and J. Wu, *Eur. J. Pharm. Sci.*, 2019, **139**, 105036.

195 G. Wang, X. Gao, G. Gu, Z. Shao, M. Li, P. Wang, J. Yang, X. Cai and Y. Li, *Int. J. Nanomed.*, 2017, **12**, 3591–3603.

196 S. Mahati, X. Fu, X. Ma, H. Zhang and L. Xiao, *Front. Mol. Biosci.*, 2021, **8**, 738219.

197 A. Varshney, J. Panda, A. Singh, N. Yadav, C. Bihari, S. Biswas, S. Sarin and V. Chauhan, *Hepatology*, 2018, **67**, 1392–1407.

198 Y. Mo, L. He, Z. Lai, Z. Wan, Q. Chen, S. Pan, L. Li, D. Li, J. Huang, F. Xue and S. Che, *Artif. Cells, Nanomed., Biotechnol.*, 2019, **47**, 2830–2837.

199 D. Singh and M. Singh, *Pharmaceutics*, 2021, **13**.

200 R. Finn, S. Qin, M. Ikeda, P. Galle, M. Ducreux, T. Kim, M. Kudo, V. Breder, P. Merle, A. Kaseb, D. Li, W. Verret, D. Xu, S. Hernandez, J. Liu, C. Huang, S. Mulla, Y. Wang, H. Lim, A. Zhu and A. Cheng, *N. Engl. J. Med.*, 2020, **382**, 1894–1905.

201 A. El-Khoueiry, B. Sangro, T. Yau, T. Crocenzi, M. Kudo, C. Hsu, T. Kim, S. Choo, J. Trojan, T. Welling, T. Meyer, Y. Kang, W. Yeo, A. Chopra, J. Anderson, C. Dela Cruz, L. Lang, J. Neely, H. Tang, H. Dastani and I. Melero, *Lancet*, 2017, **389**, 2492–2502.

202 R. Vaddepally, P. Kharel, R. Pandey, R. Garje and A. Chandra, *Cancers*, 2020, **12**.

203 N. Qiang, L. Wei, Y. Tao, W. Jin, Y. Bin and Z. DingHua, *Biomed. Mater.*, 2022, **17**, 025015.

204 C. An, W. Hu, J. Gao, B. Ju, P. Obeidy, Y. Zhao, X. Tu, W. Fang, L. Ju and W. Chen, *Nano Lett.*, 2020, **20**, 5133–5140.

205 O. Helm, J. Held-Feindt, E. Grage-Griebenow, N. Reiling, H. Ungefroren, I. Vogel, U. Krüger, T. Becker, M. Ebsen, C. Röcken, D. Kabelitz, H. Schäfer and S. Sebens, *Int. J. Cancer*, 2014, **135**, 843–861.

206 S. Bai, Z. Lu, Y. Jiang, X. Shi, D. Xu, Y. Shi, G. Lin, C. Liu, Y. Zhang and G. Liu, *ACS Nano*, 2022, **16**, 997–1012.

207 T. Wang, J. Zhang, T. Hou, X. Yin and N. Zhang, *Nanoscale*, 2019, **11**, 13934–13946.

208 Q. Zhao, Y. Wang, B. Zhao, H. Chen, Z. Cai, Y. Zheng, Y. Zeng, D. Zhang and X. Liu, *Nano Lett.*, 2022, **22**, 2048–2058.

